© 2014. Published by The Company of Biologists Ltd | Journal of Cell Science (2014) 127, 147–157 doi:10.1242/jcs.133983

RESEARCH ARTICLE

Lamins are rapamycin targets that impact human longevity: a study in centenarians

Giovanna Lattanzi[1,2,*], Michela Ortolani[1], Marta Columbaro[2], Sabino Prencipe[1,3], Elisabetta Mattioli[1,2], Catia Lanzarini[4], Nadir M. Maraldi[1,2,3], Vittoria Cenni[1,2], Paolo Garagnani[4], Stefano Salvioli[4], Gianluca Storci[4], Massimiliano Bonafè[4], Cristina Capanni[1,2] and Claudio Franceschi[4]

ABSTRACT

The dynamic organisation of the cell nucleus is profoundly modified during growth, development and senescence as a result of changes in chromatin arrangement and gene transcription. A plethora of data suggests that the nuclear lamina is a key player in chromatin dynamics and argues in favour of a major involvement of prelamin A in fundamental mechanisms regulating cellular senescence and organism ageing. As the best model to analyse the role of prelamin A in normal ageing, we used cells from centenarian subjects. We show that prelamin A is accumulated in fibroblasts from centenarians owing to downregulation of its specific endoprotease ZMPSTE24, whereas other nuclear envelope constituents are mostly unaffected and cells do not enter senescence. Accumulation of prelamin A in nuclei of cells from centenarians elicits loss of heterochromatin, as well as recruitment of the inactive form of 53BP1, associated with rapid response to oxidative stress. These effects, including the prelamin-A-mediated increase of nuclear 53BP1, can be reproduced by rapamycin treatment of cells from younger individuals. These data identify prelamin A and 53BP1 as new targets of rapamycin that are associated with human longevity. We propose that the reported mechanisms safeguard healthy ageing in humans through adaptation of the nuclear environment to stress stimuli.

KEY WORDS: Centenarian, Prelamin A, Lamins, 53BP1, Chromatin organisation, Rapamycin

INTRODUCTION

Profound changes in nuclear organisation and chromatin remodelling occur in senescent cells. Indeed, heterochromatin foci (senescence-associated heterochromatin foci) or loss of heterochromatin have been observed during cellular ageing, under different experimental conditions (Di Micco et al., 2011; Kosar et al., 2011; Sikora et al., 2011). Moreover, changes in DNA methylation have been associated with ageing and the rate of methylation decline appears to be related to longevity (Koch et al., 2012; Muñoz-Najar and Sedivy, 2011). In addition, it has been widely reported that the histone methylation pattern is profoundly modified in ageing cells (Han and Brunet, 2012; Schellenberg et al., 2011).

In recent years, the composition of the nuclear envelope has gained interest for researchers involved in ageing studies. Indeed, three different diseases of accelerated ageing have been associated with defects of the nuclear lamina. They include Hutchinson–Gilford progeria syndrome (HGPS), Mandibuloacral Dysplasia (MADA and MADB) and atypical-Werner syndrome (Maraldi et al., 2011). These diseases are caused by accumulation of the precursor protein of lamin A, one major constituent of the lamina meshwork, formed by A- and B-type lamins. Prelamin A is transcribed from the *LMNA* gene and undergoes post-translational processing, leading to transient production of different intermediates, including farnesylated full-length prelamin A and carboxymethylated prelamin A (Lattanzi, 2011). The latter form is accumulated in laminopathies resulting in premature ageing (Maraldi and Lattanzi, 2007). At the cellular level, accumulation of farnesylated prelamin A is associated with nuclear enlargement, heterochromatin loss and euchromatin dispersion, increase in reactive oxygen species (ROS) (Richards et al., 2011) and activation of the p53 pathway (Muteliefu et al., 2012). A physiological role of prelamin A in muscle and adipose tissue differentiation (Capanni et al., 2005; Mattioli et al., 2011) and smooth muscle cell ageing has been reported (Ragnauth et al., 2010). However, prelamin-A-dependent mechanisms are mostly related to its effect on chromatin dynamics (Maraldi and Lattanzi, 2007). Although farnesylated prelamin A has been shown to elicit heterochromatin loss, the non-farnesylated isoform causes formation of heterochromatic foci (Lattanzi, 2011; Lattanzi et al., 2007; Maraldi et al., 2011).

Here, we aimed to analyse the role of prelamin A in chromatin dynamics associated with normal ageing, by using cells from centenarian subjects (skin fibroblasts from individuals aged 95–105 years, here referred to as CE), who constitute a useful model in the search for traits associated with longevity (Cevenini et al., 2008). We show that accumulation of prelamin A and loss of heterochromatin occur in CE fibroblasts and this is associated with nuclear import of 53BP1, an event that is triggered by inhibition of prelamin A processing and rapamycin treatment (Bandhakavi et al., 2010; Wilkinson et al., 2012). Nuclear accumulation of 53BP1 along with increased accessibility of DNA-damage sites elicited by chromatin de-condensation, corresponds to a rapid response of CE cells to stress-induced DNA damage. We propose that these prelamin-A-linked mechanisms contribute to safeguard cell survival and healthy ageing in humans.

[1]National Research Council of Italy, Institute of Molecular Genetics, Unit of Bologna IOR, 40136 Bologna, Italy. [2]Rizzoli Orthopaedic Institute, Laboratory of Musculoskeletal Cell Biology, 40136 Bologna, Italy. [3]University of Bologna, Department of Biomedical Sciences, DIBINEM, 40126 Bologna, Italy. [4]Department of Experimental, Diagnostic and Specialty Medicine, Alma Mater Studiorum, University of Bologna, 40126 Bologna, Italy.

*Author for correspondence (giovanna.lattanzi@cnr.it)

Received 26 April 2013; Accepted 3 October 2013

Journal of Cell Science

Journal of Cell Science (2014) 127, 147–157 doi:10.1242/jcs.133983

RESULTS

Fibroblasts from centenarians are not senescent

To evaluate the proliferation rate of CE fibroblasts, we performed immunolabelling with anti-Ki67 antibody in cells from young (YO, aged 8–35 years), old (OD, aged 65–80 years) or centenarian subjects (CE, aged 95–105 years) at passage 6 (supplementary material Table S1). The majority of CE nuclei were positive for Ki67 (Fig. 1A), showing that fibroblasts were proliferating. By contrast, more than 50% of OD fibroblasts were negative for Ki67. A high percentage of Ki67-positive OD or CE nuclei showed staining of nucleoli and absent nucleoplasmic labelling. This pattern is typical of S-phase, thus a delayed S-phase occurs in OD and CE cells (Fig. 1A,C). Moreover, the senescence marker β-galactosidase (β-gal) stained less than 40% of CE fibroblasts, whereas about 80% of OD fibroblasts were positive for β-gal staining (Fig. 1B,C). OD fibroblasts reached replicative senescence very early (passage 7.5±2.3), whereas CE fibroblasts reached replicative senescence much later (passage 17.3±4.6) and were similar to YO cells (passage 20.5±3.3). Thus, we concluded that, in the case of CE fibroblasts, we were dealing with a population that although they were derived from very old individuals still presented features typical of young cells. The maintenance of a 'young-like phenotype' in CE fibroblasts, including replicative activity (Matarrese et al., 2012; Tesco et al., 1998), expression of PARP isoforms (Chevanne et al., 2007) and the molecular composition of potassium channels, has been previously reported (Zironi et al., 2010).

Prelamin A is accumulated in fibroblasts from centenarians

The composition of the nuclear lamina and the presence of wild-type prelamin A in CE cells have not been determined previously. We therefore analysed prelamin A accumulation in CE versus OD or YO fibroblasts at different passage numbers in culture, using three different anti-prelamin A antibodies (Fig. 2). At low population doublings, prelamin A accumulation did not occur in any of the examined cell cultures (Fig. 2A,B). Prelamin A accumulated in the nuclear rim of OD and CE nuclei around passages 6–8 (Fig. 2A,B). However, in OD fibroblasts, low levels of prelamin A were detected, whereas significantly higher prelamin A fluorescence intensity was measured in CE cells (Fig. 2B, right panel). Low levels of prelamin A staining were also observed in YO cells around passages 18–25 (Fig. 2B).

Prelamin A was detected in fibroblasts using a variety of antibodies (supplementary material Table S2). Whereas antibody 1188-1, which has the highest affinity for non-farnesylated prelamin A, faintly stained OD nuclei, but not YO or CE nuclei (Fig. 2A), farnesylated prelamin A (Dominici et al., 2009) was clearly detected in CE nuclei. In YO, OD or CE fibroblasts, we did not observe expression of the alternatively spliced prelamin A form called progerin, which accumulates in HGPS cells (Fig. 2A,C). Western blot analysis confirmed the above mentioned results (Fig. 2C). By using a new anti-prelamin-A antibody directed to the last 20 amino acids of full-length prelamin A, we were able to detect both farnesylated and non-farnesylated prelamin A in western blot analysis (Fig. 2C, second row).

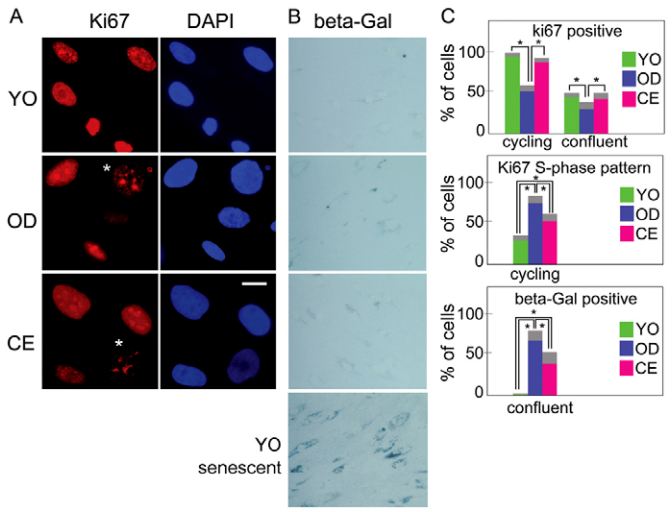

Fig. 1. CE fibroblasts are not senescent cells. (A) Immunofluorescence staining of YO, OD or CE fibroblasts using anti-Ki67 antibody (red). Cells were used at passage 6. Nuclei are counterstained with DAPI. Asterisks indicate S-phase staining pattern of Ki67. Scale bar: 10 µm. (B) β-galactosidase (beta-Gal) staining of YO, OD or CE fibroblasts. YO senescent fibroblasts at passage 35 are stained as positive control (YO senescent). (C) Quantitative evaluation of the results obtained in triplicate samples from six different subjects is reported in the graphs as means (coloured bars) ± s.d. (grey bars). Confluent (confluent) or cycling cell cultures (cycling) were examined. Significantly different values ($P<0.05$) with respect to YO or OD are indicated by asterisks.

Lamin B1 and SUN1 in nuclei of cells from centenarians

Next, we examined two nuclear envelope constituents known to interact with prelamin A under normal or pathological conditions and implicated in cellular senescence: the major nuclear lamina protein, lamin B1 (Barascu et al., 2012; Shimi et al., 2011) and the nuclear envelope protein SUN1 (Mattioli et al., 2011). Lamin B1 was downregulated in enlarged OD nuclei, whereas it was expressed at levels that were comparable to controls in the majority of YO, OD or CE cells (Fig. 2A). The western blot analysis showed a slight (but not significant) reduction of lamin B1 levels in lysates from OD fibroblasts, which could be consistent with their senescent phenotype (Fig. 2C). The prelamin A binding partner SUN1 was upregulated in CE, but not in OD nuclei (Fig. 2A,C). The latter data support the link between accumulation of farnesylated prelamin A and recruitment of SUN1 to the nuclear envelope, as previously shown in HGPS cells (Haque et al., 2010) and normal human muscle (Mattioli et al., 2011). Moreover, given that recent data have clearly shown downregulation of lamin B1 in oncogene-induced cellular senescence and upregulation of lamin B1 in cells subjected to oxidative stress (Barascu et al., 2012; Columbaro et al., 2013; Dreesen et al., 2013; Freund et al., 2012; Shimi et al., 2011), the evidence that lamin B1 is not significantly affected in CE fibroblasts (Fig. 2A,C) supports the notion that these cells maintain a 'young-like phenotype'.

ZMPSTE24 is downregulated in cells from centenarians

Western blot analysis showed moderate reduction of ZMPSTE24 protein levels in CE cellular lysates (Fig. 2C). Thus, in the search for a possible mechanism of prelamin A accumulation in CE fibroblasts, we tested *LMNA* and *FACE1/ZMPSTE24* expression by real-time RT-PCR. Whereas expression of *LMNA* did not change in OD or CE fibroblasts compared with YO fibroblasts (Fig. 2D), *FACE1* was significantly downregulated in CE cells at passage 6, but its expression was not reduced in OD fibroblasts (Fig. 2E). Importantly, downregulation of ZMPSTE24 appears to

Journal of Cell Science (2014) 127, 147–157 doi:10.1242/jcs.133983

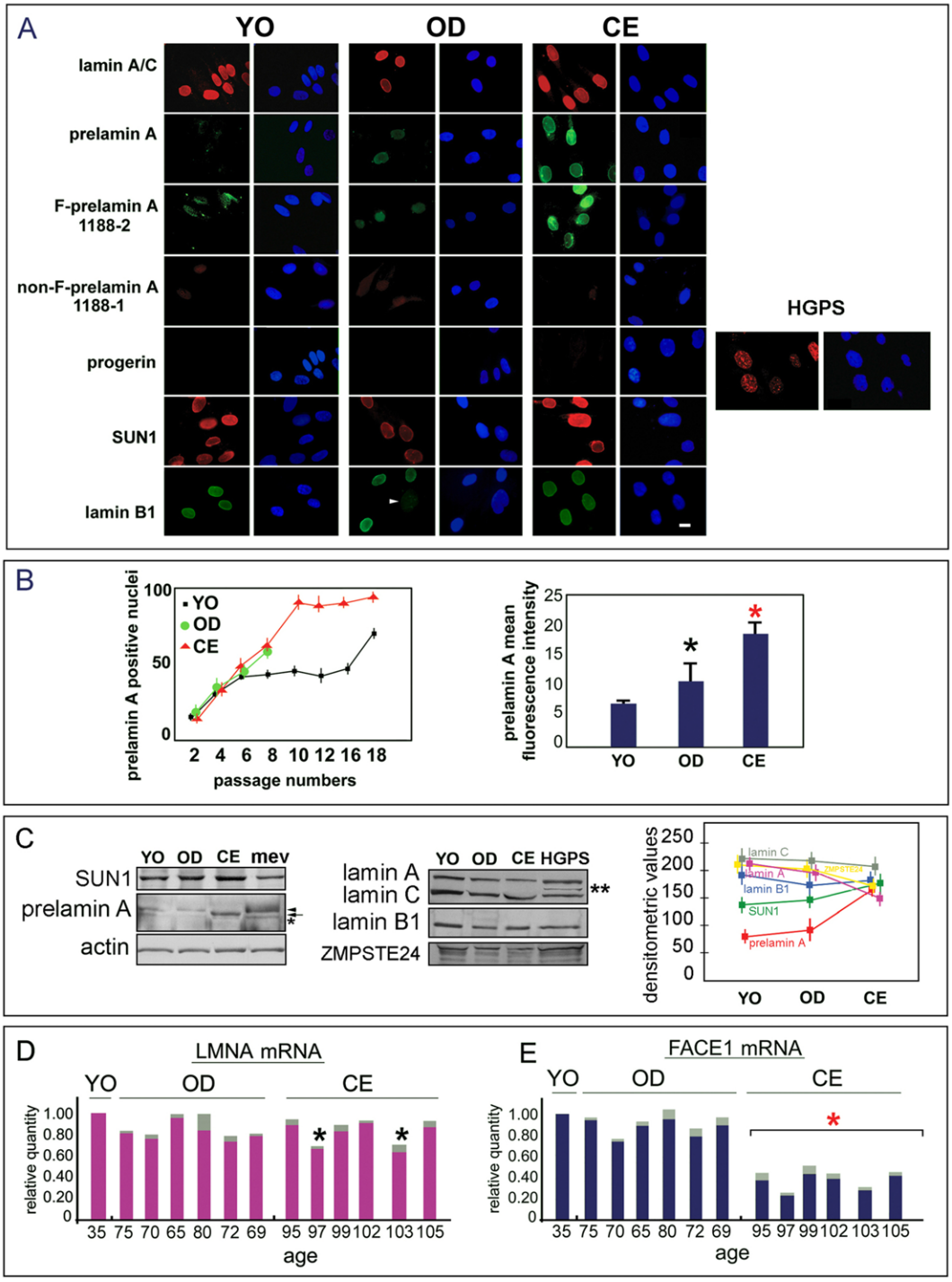

Fig. 2. Prelamin A is accumulated in CE fibroblasts. (A) Immunofluorescence staining of YO, OD or CE fibroblasts at passage 8 using anti-lamin A/C Sc-6215 (lamin A/C), anti-prelamin A Sc-6214 (prelamin A), anti-farnesylated prelamin A (F-prelamin A 1188-2), anti-non-farnesylated prelamin A (non-F-prelamin A 1188-1), progerin, SUN1 or lamin B1 antibody. Nuclei counterstained with DAPI (blue) are shown on the right. Scale bar: 10 μm. HGPS fibroblasts (HGPS) were used as positive control for progerin staining. An OD nucleus with low lamin B1 levels, which is probably a senescent cell nucleus, is indicated by an arrowhead. (B) Percentage of prelamin A (Sc-6214)-positive nuclei in YO, OD or CE fibroblasts at different passage numbers (left). The meanfluorescence intensity of prelamin A (Sc-6214) in YO, OD or CE fibroblasts at passage 8 was measured and values are plotted (right). 200 nuclei were scored in each labelled sample. (C) Western blot analysis of cell lysates from YO, OD or CE performed using anti-SUN1, anti-prelamin A (anti-prelamin A 3, supplementary material Table S2), anti-lamin A/C, anti-lamin B1 or anti-ZMPSTE24 antibodies. In the prelamin A panel, the arrowhead indicates non-farnesylated prelamin A [obtained in a mevinolin-treated YO sample (mev)], the arrow indicates fast-migrating farnesylated prelamin A band. The asterisk indicates lamin A band. The double asterisk in the lamin A/C panel indicates progerin band. Actin staining is reported as loading control. Densitometric values are reported in the graph as means ± s.d. of three different experiments performed using three cell cultures from different donors. (D) *LMNA* mRNA expression in YO, OD and CE fibroblasts at passage 6. (E) *FACE1* mRNA expression in YO, OD or CE fibroblasts at passage 6. mRNA expression was measured in triplicate samples from six different donors. $2^{-\Delta\Delta CT}$ values are reported relative to control samples. Statistical analysis was performed using Student's *t*-test, s.d. is represented by the grey bars. *$P<0.001$ (significant versus YO values); *$P<0.001$ with red asterisk (significant versus both YO and OD values).

Journal of Cell Science

Journal of Cell Science (2014) 127, 147–157 doi:10.1242/jcs.133983

be a feature of ageing cells (Ukekawa et al., 2007), including those from vascular smooth muscle (Liu et al., 2013; Ragnauth et al., 2010). However, because ZMPSTE24 was not downregulated in OD fibroblasts, some effect on prelamin A farnesylation and/or stability appears to be more likely in those cells. Furthermore, the reduction of ZMPSTE24 mRNA and protein levels observed here in CE cells cannot be the sole mechanism leading to prelamin A accumulation, which could also be due to reduced enzymatic activity.

Prelamin A is accumulated in cells subjected to stress

On the basis of our observations and published data (Ragnauth et al., 2010), we hypothesised that CE cells might have developed a mechanism implicating prelamin A accumulation to counteract repeated stress stimuli. To test this hypothesis, we treated YO, OD or CE fibroblasts with H_2O_2 and examined ZMPSTE24 expression. In all the examined cell cultures, slight downregulation of ZMPSTE24 was observed (supplementary material Fig. S1). However, prelamin A was significantly increased in YO and OD fibroblasts treated with H_2O_2 and slightly increased in CE cells (Fig. 3A–E and supplementary material Fig. S2). Moreover, prelamin A was accumulated in the majority of YO cells subjected to replicative stress (Fig. 3A–C). The different reactivity of prelamin A antibodies observed in western blot analysis further showed that different prelamin A forms are accumulated in YO, OD or CE cells upon oxidative stress (Fig. 3D). Importantly, prelamin A levels decreased after H_2O_2 recovery to levels comparable to the corresponding untreated sample in YO, OD and CE cellular lysates (Fig. 3D,E).

Heterochromatin loss in fibroblasts from centenarians

To obtain detailed information on chromatin modifications occurring in CE cells or in cells subjected to stress stimuli, we performed an ultrastructural analysis. In YO fibroblasts a uniform distribution of heterochromatin at the nuclear periphery was observed, whereas all CE nuclei that we observed were enlarged and presented complete heterochromatin loss and euchromatin dispersion (Fig. 4A,F). Nuclear morphology was altered in a minor percentage OD fibroblasts, but some heterochromatin foci were maintained at the nuclear periphery (82% of fibroblasts) and euchromatin was well preserved (Fig. 4A,F).

Cytoplasm reorganisation in fibroblasts from centenarians

Relevant changes in cytoplasmic structures were detected in a percentage of OD cells and in the vast majority of CE cells. Rough endoplasmic reticulum was enriched in 20% of OD fibroblasts (Fig. 4B,G), whereas profound changes in intermediate filament organisation were found in the majority of CE cells (Fig. 4B,C,H). Immunofluorescence analysis of vimentin showed altered organisation of filaments in CE fibroblasts, with ruptures and increased thickness (Fig. 4C,H). Modification of vimentin structure leading to formation of thick filaments in skin fibroblasts from old individuals is associated with increased glycation of the protein and loss of contractile abilities of cells (Kueper et al., 2007).

Chromatin and cytoplasm modifications in cells subjected to stress

As expected, euchromatin dispersion was also observed in YO cells induced to accumulate farnesylated prelamin A by drug

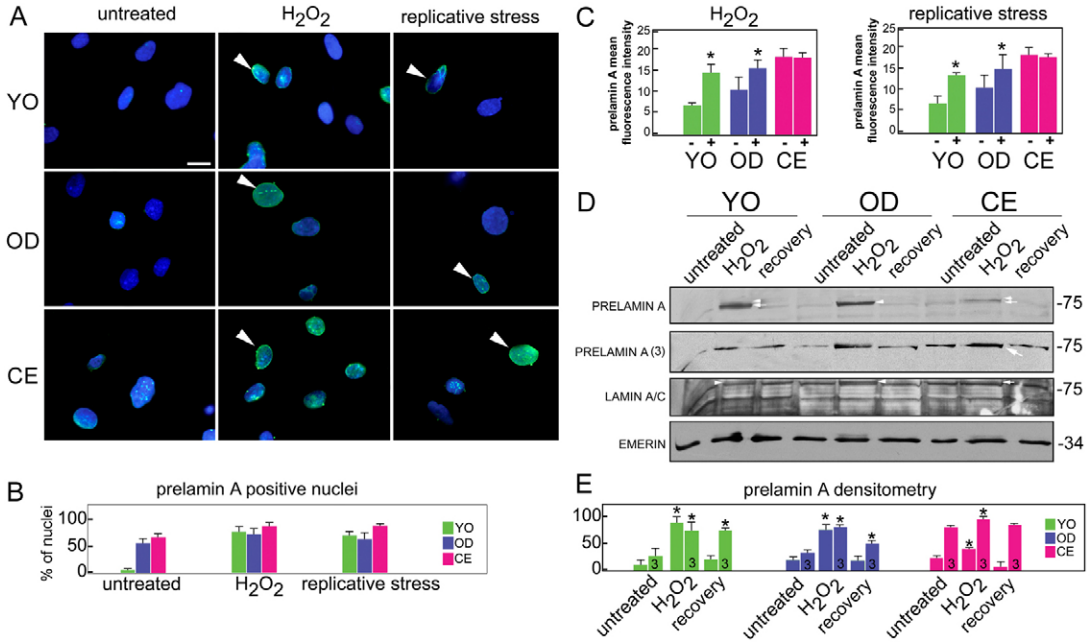

Fig. 3. Stress stimuli induce accumulation of prelamin A. (A) YO, OD or CE cells subjected to oxidative stress for 24 hours (H_2O_2) or replicative stress (repeated passages, 18, 16 or 18 for YO, OD, CE, respectively) were labelled for prelamin A (Santa Cruz SC-6214, green). Nuclei were counterstained using DAPI. Scale bar: 10 μm. Arrowheads indicate representative nuclei that accumulate prelamin A. (B) Quantification of data as a percentage of labelled nuclei ± s.d. 100 nuclei were counted in each sample. (C) Mean fluorescence intensity of prelamin A staining measured by NIS software. Values are means ± s.d. of six measurements preformed in triplicate experiments. (D) Western blot analysis of prelamin A, lamin A/C and emerin (used as a loading control) in fibroblasts left untreated (untreated), treated with H_2O_2 (H_2O_2) or treated with H_2O_2 and allowed to recover for 24 hours (recovery). Prelamin A was detected using Sc-6214 antibody (prelamin A, first row) or new anti-prelamin A-3 antibody [prelamin A (3)]. Slow-migrating bands corresponding to non-farnesylated prelamin A are indicated by arrowheads; fast-migrating bands corresponding to farnesylated prelamin A are indicated by arrows. (E) Densitometric analysis showing values relative to prelamin A bands detected using Sc-6214 antibody (unlabelled bars) or anti-prelamin A(3) antibody (bars labelled 3).

Journal of Cell Science (2014) 127, 147–157 doi:10.1242/jcs.133983

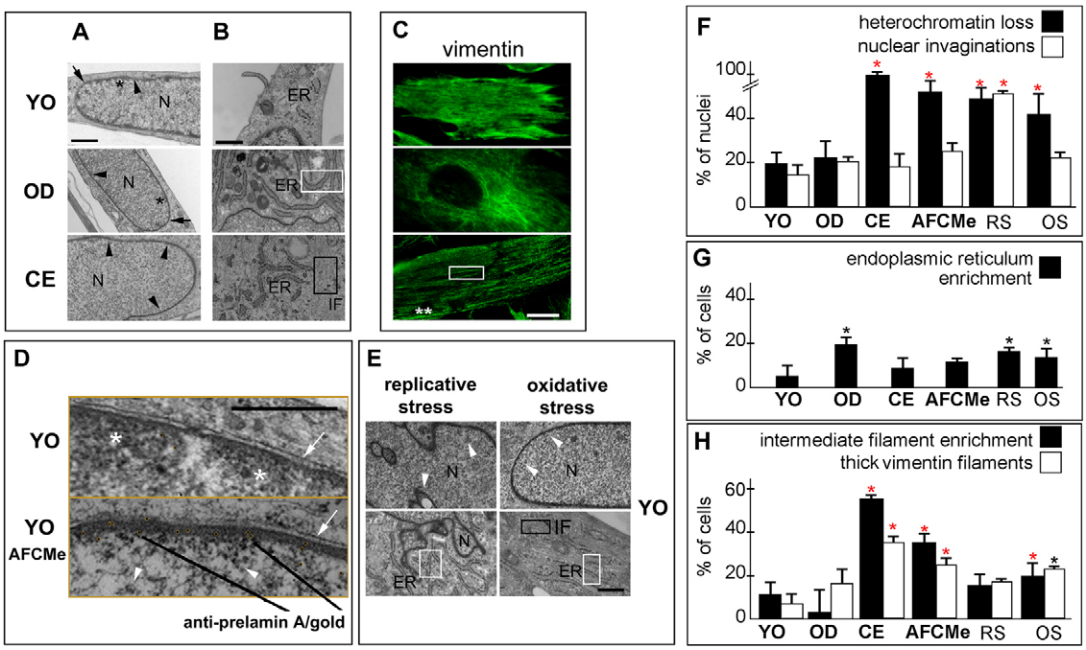

Fig. 4. Heterochromatin loss and cytoplasm modification in CE fibroblasts. (A) Ultrastructural analysis of untreated YO, OD or CE fibroblasts showing complete heterochromatin loss in CE nuclei and focal loss in OD nuclei. (B) Ultrastructural analysis of cytoplasmic structures in YO, OD or CE fibroblasts showing ER increase in OD cells (white rectangle) and increased intermediate filament network (black rectangle) in CE. (C) Vimentin immunofluorescence labelling of YO, OD or CE fibroblasts. Thick vimentin filaments (white rectangle) and filament rupture (double asterisk) are observed in CE. (D) Immunogold labelling of YO fibroblasts left untreated (YO, top) or AFCMe-treated (YO AFCMe, bottom) to induce farnesylated prelamin A. Gold-labelled anti-prelamin A (particles highlighted in yellow circles) and euchromatin dispersion are detectable. (E) YO fibroblasts subjected to replicative or oxidative stress showing heterochromatin loss (top row) and active ER (bottom row). N, nucleus; ER, endoplasmic reticulum; IF, intermediate filaments. Arrows indicate the nuclear membrane, asterisks show heterochromatin domains, arrowheads indicate areas devoid of peripheral heterochromatin. (F–H) Quantitative analysis of data shown in A–E. *$P<0.05$ by Student's *t*-test relative to YO only; *$P<0.05$ with red asterisks, relative to YO and OD. Scale bars: 1 μm (A,B,E), 10 μm (C), 500 nm (D).

treatment [see the Materials and Methods, Fig. 4D,F (YO AFCMe)]. Moreover, YO nuclei subjected to stress stimuli showed chromatin organisation that was comparable with the absence of heterochromatin areas in CE nuclei (Fig. 4E,F). However, nuclei of cells subjected to replicative stress showed envelope invaginations (Fig. 4E,F). The cytoplasm of cells subjected to oxidative or replicative stress showed increased endoplasmic reticulum (Fig. 4E,G), as also observed in OD fibroblasts, and minor changes in intermediate filaments (Fig. 4E,H).

Chromatin dynamics suggested by the ultrastructural studies was consistently supported by the immunofluorescence analysis of histone methylation status (supplementary material Fig. S3). In fact, clusters of trimethyl-H3K9, a marker of constitutive heterochromatin, were considerably reduced in CE fibroblasts with respect to YO cells at the same passage number in culture (supplementary material Fig. S3A,C), as well as in YO fibroblasts subjected to stress (supplementary material Fig. S3B,C). However, the total amount of trimethyl-H3K9, as determined by western blot analysis, was slightly affected (supplementary material Fig. S3D).

Thus, we concluded that changes in heterochromatin arrangement, associated with prelamin A accumulation, are a common feature of CE fibroblasts and cells subjected to stress and could be part of a mechanism aimed at reorganisation of chromatin domains and reprogramming of transcriptional and translational pathways. The presence of an enriched rough endoplasmic reticulum in both OD fibroblasts and YO fibroblasts subjected to stress stimuli suggested that cells were able to activate the transcriptional machinery to fulfil increased need for protein synthesis determined by stress conditions (De Cecco et al., 2011). However, CE fibroblasts seemed to be in a steady state, not requiring activation of ribosomal activity.

Low basal level of DNA damage in CE cells

Because oxidative stress induces DNA double-strand breaks, we tested the hypothesis that chromatin relaxation (Krishnan et al., 2011) in CE cells accumulating prelamin A could increase accessibility of sites of DNA damage and favour DNA repair. A key player in the DNA-damage response is 53BP1, which has a role in non-homologous end joining (NHEJ) of damaged DNA strands (Brachner and Foisner, 2011). 53BP1 is a lamin-A/C binding partner, and downregulation of the *Lmna* gene abrogates 53BP1 recruitment (Gonzalez-Suarez et al., 2011). Surprisingly, we found that an increased amount of 53BP1 is recovered in CE nuclei with respect to YO or OD cells (Fig. 5A,C). However, the active phosphorylated form is not detectable under basal conditions, and DNA damage foci do not accumulate in CE nuclei (Fig. 5B). Thus, CE cells show a lower basal level of DNA damage than the OD cells, which accumulate active 53BP1 foci (Fig. 5B,C). The latter observation is further supported by the low γH2AX levels measured in CE cells (supplementary material Fig. S4). However, γH2AX is upregulated in OD, but downregulated in those OD nuclei that have probably reached replicative senescence (supplementary material Fig. S4) (Atsumi et al., 2011). These results suggest that 53BP1-mediated DNA repair mechanisms, including NHEJ, are selected in CE cells.

Journal of Cell Science (2014) 127, 147–157 doi:10.1242/jcs.133983

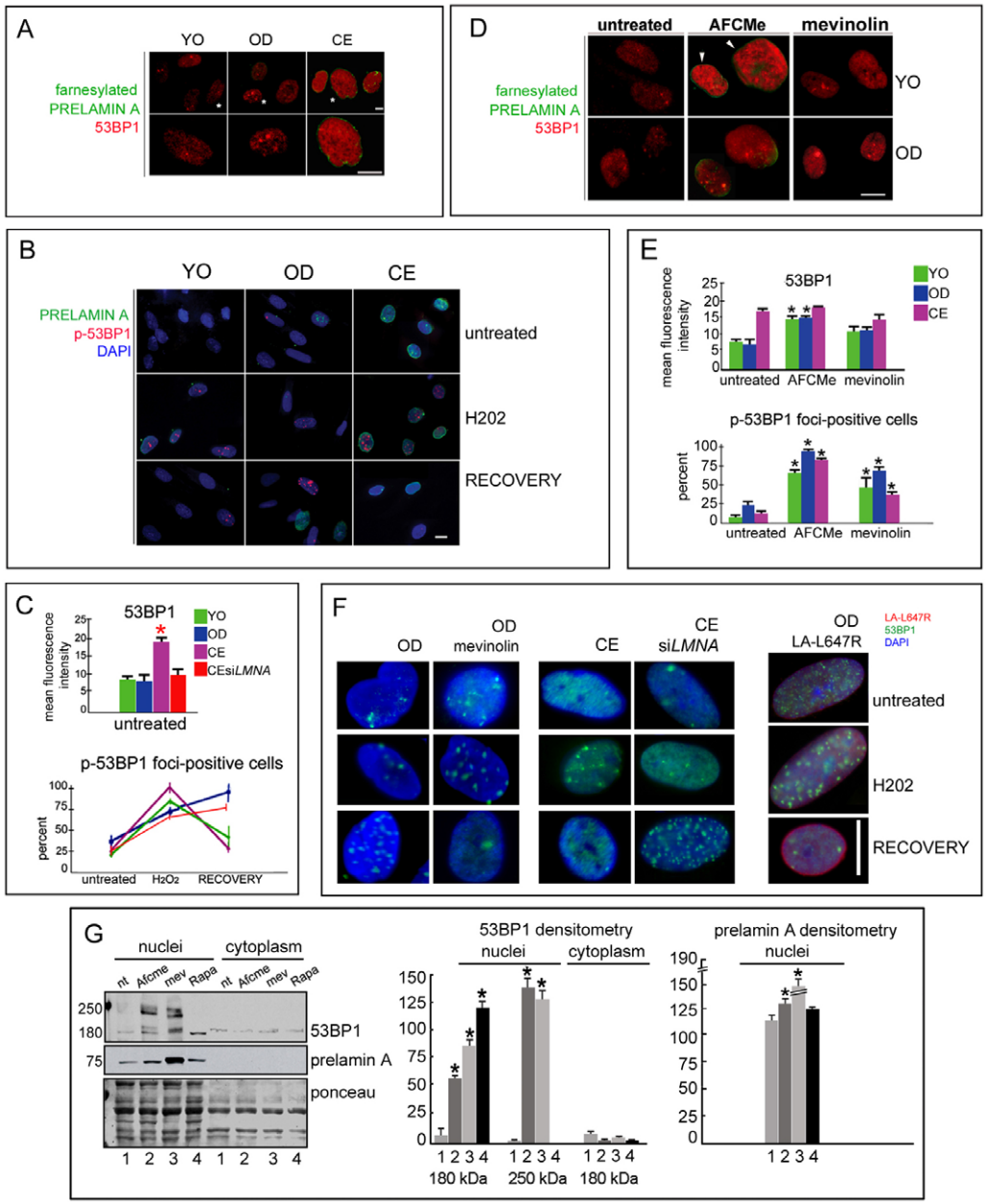

Fig. 5. 53BP1 nuclear recruitment and rapid oxidative stress response in CE fibroblasts. (A) Prelamin A and native 53BP1staining in YO, OD and CE cells. FITC-conjugated secondary antibody (green) was used to detect prelamin A labelled by Sc-6214 antibody. 53BP1 was detected using TRITC-conjugated anti-rabbit IgG (red) to reveal the anti-53BP1 antibody. Nuclei indicated by white asterisks are shown at higher magnification in the bottom row. (B) Prelamin A (green) and p53BP1 staining (p-53BP1, red) in YO, OD and CE cells performed in untreated fibroblasts (untreated), fibroblasts after 24 hours of H_2O_2 treatment (H_2O_2) and fibroblasts after 24 hour recovery from H_2O_2 treatment (recovery). Nuclei were counterstained with DAPI. (C) The top graph shows the mean fluorescence intensity measurement of 53BP1 in the nuclei shown in A and in si*LMNA* CE fibroblasts. Triplicate measurements were performed in separate experiments using the NIS software. The bottom graph reports the number of p53BP1-foci-positive cells in each sample shown in B and in si*LMNA* CE fibroblasts. Triplicate counts of separate experiments were performed using the NIS software. Values are reported as means ± s.d. Statistically significant difference ($P<0.05$ according to the Student's *t*-test) between CE values and any other sample are indicated by a red asterisk. (D) Prelamin A accumulation and nuclear 53BP1 increase (arrowheads) in AFCMe-treated (AFCMe) or mevinolin-treated (mevinolin) YO or OD fibroblasts observed by immunofluorescence analysis. Farnesylated prelamin A was labelled using anti-prelamin A 1188-2 (green), 53BP1 was labelled using monoclonal anti-53BP1 (red). (E) The top graph shows the mean fluorescence intensity measurement of 53BP1 in untreated nuclei (untreated) or in the nuclei of cells subjected to AFCMe or mevinolin. Triplicate measurements were performed in separate experiments using the NIS software. The bottom graph reports the number of p53BP1-foci-positive cells in each sample. Triplicate counts of separate experiments were performed using the NIS software. Values are reported as means ± s.d. *$P<0.05$ by Student's *t*-test with respect to the corresponding untreated sample. (F) Modification of prelamin A levels in OD or CE fibroblasts influences 53BP1 levels and oxidative stress response. OD, untreated OD fibroblasts; OD mevinolin, OD fibroblasts subjected to mevinolin; CE, untreated CE; CE siLMNA, CE fibroblasts transfected with si*LMNA*; OD LA-L647R, OD fibroblasts expressing farnesylated uncleavable prelamin A. Oxidative stress experiments were performed as reported for B. (G) Western blot analysis of 53BP1 in nuclear (nuclei) and cytoplasmic fractions (cytoplasm) obtained from untreated YO fibroblasts (nt) or fibroblasts subjected to AFCMe (AFCMe), mevinolin (mev) or rapamycin treatment (Rapa). Prelamin A bands were revealed using SC-6214 antibody, 53BP1 was revealed by monoclonal anti-53BP1. Molecular mass markers are in kDa. Ponceau staining (ponceau) shows equal loading of samples. 53BP1 densitometry is reported in the left graph: data are means ± s.d. of three different experiments. 180 kDa and 250 kDa band densitometric values are reported for nuclei and cytoplasm as detailed in the labels. Prelamin A densitometry is reported in the graph on the right; data are means ± s.d. of three different experiments. *$P<0.05$ by Student's *t*-test with respect to untreated samples. Scale bars: 10 μm.

Journal of Cell Science (2014) 127, 147–157 doi:10.1242/jcs.133983

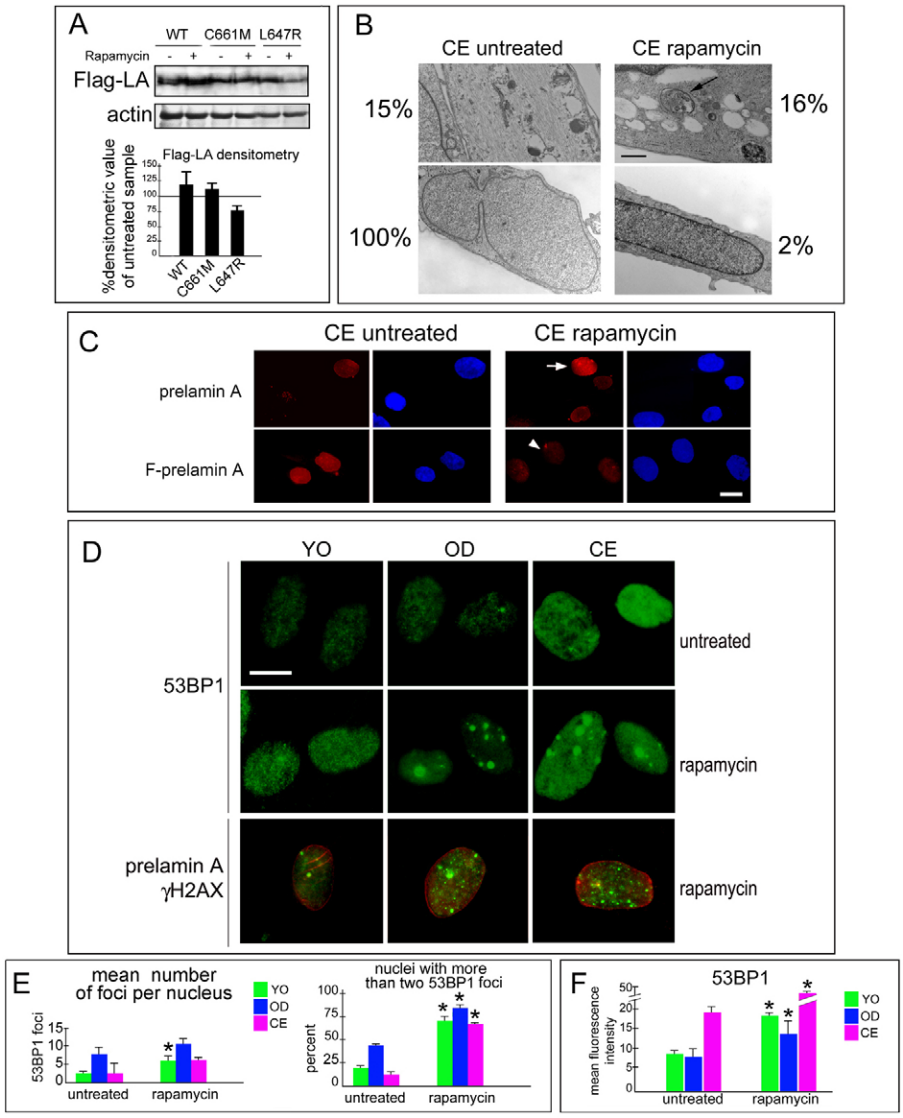

Fig. 6. Rapamycin elicits 53BP1 recruitment in the nucleus. (A) Western blot analysis of HEK293 cells expressing FLAG-prelamin A (Flag-LA) forms left untreated (−) or treated with rapamycin for 72 hours (+). WT, wild-type prelamin A, C661M, unprocessable non-farnesylated prelamin A, L647R, uncleaveable farnesylated prelamin A. Actin is reported as a loading control. Densitometric values of FLAG-LA are plotted as a percentage of the densitometric value of the corresponding untreated samples. (B) Transmission electron microscopy analysis of CE fibroblasts left untreated (CE untreated) or subjected to rapamycin treatment (CE rapamycin). 15% of CE fibroblasts showed autophagic vacuoles, whereas 16% of rapamycin-treated CE fibroblasts showed an advanced autophagic process: a well-organised autophagic vacuole is indicated by the arrow. Untreated CE nuclei showed complete heterochromatin loss, whereas rapamycin-treated cells showed heterochromatin foci in 2% of 200 examined nuclei. Percentages next to each panel show the frequency of the observed phenomena. (C) Prelamin A staining (red) in CE cells left untreated or treated with rapamycin. Prelamin A was labelled using two different antibodies: anti-prelamin A Sc- 6214 (prelamin A), anti-prelamin A 1188-2 (F-prelamin A). Staining of full-length prelamin A is increased in rapamycin-treated cells (arrow), staining of F-prelamin A is decreased (arrowhead). (D) 53BP1 staining in YO, OD or CE nuclei before (untreated) and after rapamycin treatment (rapamycin). γH2AX (green) and prelamin A (red) double-staining in YO, OD or CE nuclei after rapamycin treatment is shown in the bottom row. (E) Statistical analysis to show changes in number of 53BP1 foci per nucleus and in the percentage of nuclei with more than two 53BP1 foci. (F) Mean 53BP1 fluorescence intensity measured by NIS software is reported. *$P<0.05$ by Student's *t*-test with respect to each corresponding untreated sample. Scale bars: 1 μm (B), 10 μm (C,D).

Rapid DNA damage response in CE cells

To test whether increased 53BP1 levels in CE nuclei could favour the DNA repair activity, we treated fibroblasts with H_2O_2 to induce oxidative stress. Upon oxidative stress induction, 53BP1 foci at DNA damage sites were promptly formed in CE nuclei and recovery of DNA damage was more rapid than in YO or OD nuclei (Fig. 5B,C). These findings suggest that both chromatin dispersion and import of 53BP1 favour DNA repair mechanisms in CE fibroblasts. However, early replicative arrest, associated with unmodified chromatin status and low levels of prelamin A accumulation are characteristics that we could identify in OD cells. These observations and the fact that 53BP1 nuclear translocation was evident in CE, but not in OD fibroblasts, indicate that we are dealing with different cellular populations.

Prelamin A accumulation triggers nuclear recruitment and activation of 53BP1

Next, we wondered whether prelamin A accumulation per se could affect the amount or activity of 53BP1. Treatment of YO fibroblasts with AFCMe, a non-competitor peptide known to block ZMPSTE24-mediated endoproteolysis and induce farnesylated prelamin A accumulation (Mattioli et al., 2008), not only elicited nuclear enlargement and heterochromatin decondensation (Fig. 4D and Fig. 5D), but also caused an increase of nuclear 53BP1 (Fig. 5D,E). Moreover, the number of nuclei with 53BP1-positive foci was increased in AFCMe-treated YO and OD nuclei (Fig. 5D,E). However, treatment with mevinolin, which induces accumulation of non-farnesylated prelamin A, caused a moderate increase of 53BP1 levels in nuclei (Fig. 5D,E). To further support the involvement of prelamin A in the resistance of CE cells to oxidative stress, we downregulated *LMNA* expression in CE fibroblasts and exposed cells to oxidative stress. CE fibroblasts expressing low prelamin A levels showed slow recovery from DNA damage (Fig. 5F) and increased mortality. Conversely, expression of unprocessable prelamin A forms or mevinolin treatment increased resistance to DNA damage in OD cells subjected to oxidative stress (Fig. 5F). These results indicate that prelamin A contributes to the activation of the DNA repair machinery, by inducing both chromatin remodelling and 53BP1 nuclear recruitment, as also confirmed by the western blot analysis of subcellular fractions (Fig. 5G). However, to what extent the prelamin-A-linked increase of 53BP1 in the nucleus is due to translocation or

Journal of Cell Science (2014) 127, 147–157 doi:10.1242/jcs.133983

rather to protein stabilisation remains to be established (Gonzalez-Suarez et al., 2011).

Rapamycin affects chromatin organisation and 53BP1 nuclear import

The overall evaluation of the reported data indicates that prelamin A accumulation and 53BP1 nuclear import in the elderly are part of a defence mechanism against stress events and could contribute to lifespan extension. Because rapamycin, a drug known to extend lifespan in mouse and *C. elegans*, affects prelamin A stability (Cenni et al., 2011b; Graziotto et al., 2012) and triggers both nuclear import and activation of 53BP1 (Bandhakavi et al., 2010; Pospelova et al., 2012), we tested the effect of rapamycin in fibroblasts. As shown in Fig. 5G, rapamycin treatment increased prelamin A levels in YO fibroblasts and further enhanced levels of 53BP1. This result was quite unexpected and seemingly in disagreement with the reported effect of rapamycin on progerin (Cao et al., 2011; Cenni et al., 2011b). However, detailed analysis showed that rapamycin selectively triggers degradation of farnesylated prelamin A, whereas it enhances accumulation of non-farnesylated prelamin A (Fig. 6A).

As expected, in CE fibroblasts subjected to rapamycin, we observed an advanced autophagic process, demonstrated by the presence of well-organised autophagic vacuoles (Fig. 6B, arrow). Partial reorganisation of heterochromatin domains was observed in a low percentage of rapamycin-treated CE nuclei, as shown by electron microscopy analysis (Fig. 6B). The effects of rapamycin on prelamin A levels were consistent with the results shown in Fig. 5G and Fig. 6A (Cenni et al., 2011b; Lattanzi et al., 2007; Marmiroli et al., 2009). In fact, in YO, OD or CE fibroblasts, rapamycin elicited a moderate increase of full-length prelamin A staining, but reduced levels of farnesylated carboxymethylated prelamin A (Fig. 6C). These effects were associated with recruitment of 53BP1 in the nucleus to levels comparable to that in untreated CE cells (Fig. 6D–F). The number of nuclei with 53BP1 foci was also increased in rapamycin-treated cells, suggesting activation of the DNA repair machinery (Fig. 6D,E). Thus, we can conclude that rapamycin treatment mimics the effects observed in CE nuclei, including prelamin A accumulation and recruitment of 53BP1 and might improve genome stability, as previously shown in senescent cells (Pospelova et al., 2012).

DISCUSSION

Our study reports an unexpected function of prelamin A in 53BP1 nuclear recruitment, which we show occurs naturally in cells from 100-year-old individuals. The nuclear setting of CE fibroblasts, including the open chromatin conformation, contributes to the rapid oxidative stress response observed in those cells and to their sustained proliferation. Nevertheless, CE fibroblasts present features of cells from old individuals, such as enlarged nuclei and thickening of vimentin filaments. However, OD cells appear to be a mixed population, including mostly cells entering replicative senescence, but also some prelamin A-positive cells. We speculate that in old individuals a heterogeneous population of fibroblasts is present, which can potentially select the best phenotype to prolong survival. The delayed response to oxidative-stress-induced DNA damage observed in OD cells might in part account for the early replicative senescence reached by those cells.

Increased levels of 53BP1 in the nucleus of YO or OD cells are elicited not only by accumulation of prelamin A and 53BP1 in the nuclei of CE cells, but also by a slow-down of prelamin A maturation caused by processing inhibitors. Furthermore, stress stimuli induced accumulation of prelamin A in any cell type here examined, whereas the response of CE cells, in terms of processing of active 53BP1 foci after damage appears more rapid. This might explain in part the presence of a lower number of 53BP1 and gamma-H2AX foci in CE with respect to OD cells. Interestingly, CE fibroblasts that do not accumulate prelamin A because of knockdown of mRNA show lower levels of 53BP1 in nuclei and a stress response comparable to OD cells. Therefore, we speculate that prelamin A contributes to set a nuclear arrangement, which makes a prompt response to stress stimuli possible. Importantly, we show that γ-H2AX-mediated response to DNA damage is downregulated in CE fibroblasts, whereas nuclear 53BP1 levels are increased. Because γ-H2AX-mediated repair is associated with homologous end joining, a DNA repair mechanism that requires energy expenditure, whereas 53BP1 favours NHEJ (Gonzalez-Suarez et al., 2011), we hypothesise that a low-energy mechanism is activated in very old individuals, which allows CE cells to survive long-lasting stress. In this scenario, prelamin A might drive the option towards NEHJ. However, it has been previously shown that cells from Zmpste24$^{-/-}$ mice, which accumulate prelamin A, are more prone to DNA damage and show a delayed response (Liu et al., 2005). Moreover, it has been established that accumulation of either mutated or wild-type prelamin A in young or very young individuals elicits deleterious effects, such as in laminopathies. This is consistent with the evidence that prelamin A is a toxic molecule, which must be finely regulated and maintained below a threshold level. As shown in supplementary material Fig. S2, cells that accumulate excess levels of prelamin A exit the cell cycle and probably undergo senescence. Furthermore, it must be considered that mature lamin A, which is primarily involved in targeting active 53BP1 to DNA-damage sites (Brachner and Foisner, 2011), is not produced in Zmpste24$^{-/-}$ cells, whereas it is efficiently formed in CE cells and probably contributes to 53BP1 functionality.

Our data add to the evidence that prelamin A is accumulated in normal smooth muscle cells during ageing as an effect of *FACE1* downregulation (Ragnauth et al., 2010) and to our previously published data showing a physiological role of prelamin A (Lattanzi et al., 2007; Capanni et al., 2010; Mattioli et al., 2011). We envisage that a non-modulated, thus inappropriate, response mechanism is activated in laminopathies as a result of molecular defects. However, an appropriate mechanism of response, involving accumulation of proper levels of prelamin A, might help CE cells to survive long-lasting stress stimuli through modulation of chromatin arrangement and availability of the DNA-repair machinery. Moreover, and in agreement with the proposed protective role of lamins, it has been recently demonstrated that oxidation of cysteine residues in the lamin A tail protects cells from oxidative-stress-induced damage, whereas knockdown of lamin A accelerates ROS accumulation and causes cellular senescence (Richards et al., 2011). In this context, accumulation of proper levels of prelamin A during healthy ageing might increase the availability of mature lamin A (which can be promptly processed, without the need for transcription and translation), which could act as a sink for ROS at the nuclear envelope. Thus, lamin A appears to be involved both in the nuclear response to stress and in the reduction of stress stimuli. It is worth considering that other effects of the accumulation of prelamin A in CE cells might be relevant to the cellular phenotype and this deserves further investigation.

The number and quality of biochemical pathways that are required to downregulate *FACE1* activity and/or alter the methylation rate of prelamin A (Ibrahim et al., 2013), or even affect prelamin A stability (Bertacchini et al., 2013) and initiate accumulation in healthy individuals remain to be established. Unravelling these pathways will provide powerful tools to counteract ageing-related disorders. In this context, our study provides the first evidence that rapamycin, a drug widely investigated for its potential effects in lifespan extension, affects prelamin A levels and, as previously shown (Bandhakavi et al., 2010; Burtner and Kennedy, 2010), favours nuclear recruitment of 53BP1, thus mimicking the nuclear setting observed in CE cells. These results deserve further study, particularly in the area of understanding mTOR-dependent signalling pathways (Ramos et al., 2012), which might interfere with the regulation of prelamin A.

MATERIALS AND METHODS

Cell culture

Skin fibroblast cultures were obtained following written consent from skin biopsies of healthy patients (supplementary material Table S1) and were cultured in D-MEM plus 10% foetal calf serum and antibiotics. Cells were repeatedly subcultured to induce replicative stress. 50 µM hydrogen peroxide (H_2O_2) was added to cell cultures for 24 hours to induce oxidative stress. Recovery was measured after 24 hours after H_2O_2 removal. 5 µM rapamycin was applied to fibroblasts for 3 days. 10 µM mevinolin or 10 µM AFCMe were applied to fibroblast cultures for 24 hours before fixation to induce accumulation of non-farnesylated or farnesylated prelamin A, respectively (Dominici et al., 2009). CE fibroblasts were transfected using INGENIO reagent (MirusBio, Madison, WI) in the Amaxa nucleofector according to the manufacturer's instructions to express LA-WT (wild-type lamin A), LA-L647R (farnesylated prelamin A) (Lattanzi et al., 2007) or si*LMNA* (Santa Cruz, SC-35776). Downregulation of lamin A/C and prelamin A was measured by immunofluorescence staining of nuclei. HEK293 cells were transfected using the calcium phosphate method (Cenni et al., 2011a).

Antibodies

The antibodies used (supplementary material Table S2) were directed against: prelamin A (Santa Cruz SC-6214), lamin A/C (Santa Cruz SC-6215), prelamin A (1188-1 and 1188-2, Diatheva), prelamin A (prelamin A 3, 20 amino acids C-terminal sequence), progerin, (clone 13A4, Alexis), SUN1 (Atlas), lamin B1 (Santa Cruz SC-5614), Ki67 (Santa Cruz SC-7846), vimentin (Sigma V6630), trimethylated-H3 histone (Abcam), H3 histone (Santa Cruz), phosphorylated (Ser1778) 53BP1 (p53BP1) and 53BP1 (here referred to as 53BP1) antibodies (Cell Signaling), γ-H2AX antibody (Abcam), ZMPSTE24 antibody (Santa Cruz) and FLAG (M2, Sigma).

Immunofluorescence

Human fibroblasts were fixed in methanol at −20℃ or in paraformaldehyde at 4℃. Samples were incubated overnight with primary antibodies and for 1 hour with secondary antibodies. Cells were observed with a Nikon E 600 epifluorescence microscope equipped with a digital camera. Fluorescence intensity measurements were performed using NIS elements 2.20. Images were processed using Adobe Photoshop 7.

Gene expression

Total RNA was isolated using RNeasy Mini Kit (Qiagen, Hilden, Germany) following the manufacturer's instructions. RNA was reverse transcribed into cDNA using the High Capacity cDNA Reverse Transcription Kit (Applied Biosystems, Monza, Italy). *LMNA* or *ZMPSTE24* expression was evaluated by real-time PCR, using an Applied Biosystems StepOne thermal cycler (Applied Biosystems), by amplifying 1 µg of cDNA and TaqMan gene expression assays (Applied Biosystems). Probes and primers obtained from Applied Biosystems were: GAPDH, assay ID Hs99999905_m1, *LMNA*, assay ID Hs00153462_m1*, *ZMPSTE24*, assay ID Hs00195298_m1*. The amplification protocol was: 50℃ for 2 minutes; 95℃ for 10 minutes; 95℃ for 15 seconds, 60℃ for 1 minute, for 40 cycles. The results were calculated by the $2^{-\Delta\Delta CT}$ method or as the ratio between the gene of interest and the *GAPDH* reference gene. The experiments were performed in triplicate.

β-galactosidase staining

Cells were fixed for 3 minutes at 22℃ with 2% formaldehyde/0.2% glutaraldehyde and incubated overnight at 37℃ in 1 mg/ml X-gal, 40 mM citric acid-sodium phosphate (pH 6 or 4), 5 mM potassium ferricyanide, 5 mM potassium ferricyanide, 150 mM NaCl and 2 mM $MgCl_2$.

Biochemical analysis

Purified nuclei and cytoplasmic fractions from YO fibroblasts (Capanni et al., 2012) were lysed in RIPA buffer and subjected to western blot analysis. Proteins were separated by a 4–12% gradient SDS–PAGE. Protein bands were blotted onto a nitrocellulose membrane and subjected to immunolabelling using anti-prelamin A (Santa Cruz, sc-6214) and anti-lamin-A/C antibody (Santa Cruz, sc-6215) used at 1:100 dilution. Anti-53BP1 antibody (Cell Signaling) was applied overnight at 1:50 dilution. Other primary antibodies were applied for 1 hour at room temperature. Peroxidase-conjugated secondary antibodies (Sigma) were applied for 20 minutes at room temperature. Immunoblotted bands were revealed by the Amersham ECL detection system.

Electron microscopy

Cell pellets were fixed with 2.5% glutaraldehyde, 0.1 M cacodylate buffer, pH 7.3. After post-fixation with 1% osmium tetroxide in cacodylate buffer, pellets were embedded in Epon resin. Ultrathin sections were stained with uranyl acetate and lead citrate and observed at 0° tilt angle with a Philips EM 400 transmission electron microscope, operated at 100 kV. At least 200 nuclei per sample were observed. Immunogold labelling of ultrathin sections was performed as previously described (Mattioli et al., 2008).

Statistical analysis

Statistical analysis was performed using the Student's *t*-test. Experiments were done in triplicate and differences were considered statistically significant at $P<0.05$.

Acknowledgements

The technical support of A. Valmori, S. Grasso and D. Zini is gratefully acknowledged.

Competing interests

The authors declare no competing interests.

Author contributions

G.L.: study design and discussion of results, manuscript writing; M.O.: cell culture, RT-PCR, M.C.: electron microscopy analysis; S.P., E.M., G.S.: immunofluorescence staining, cell biology studies; C.L., S.S.: cell culture establishment and characterisation, proliferation analysis; N.M.M.: discussion of results, fund raising; V.C., C.C.: molecular biology, cell biology experiments, image analysis, statistical analysis; P.G., C.F., M.B.: study design, discussion of results.

Funding

This work was supported by the EU COST Action BM1002 'Nanomechanics of intermediate filament networks', A.I.Pro.Sa.B., Italy and Italian MIUR PRIN 2008 to G.L.; Italian Firb 2010 '5 per mille', 2010 Rizzoli and 'Fondazione Carisbo' to N.M.M. European Union's Seventh Framework Programme (FP7/2007-2011) [grant number 259679] (IDEAL) and MiUR Prin 2009 to C.F.; Roberto and Cornelia Pallotti Legacy for cancer research to S.S.

Supplementary material

Supplementary material available online at
http://jcs.biologists.org/lookup/suppl/doi:10.1242/jcs.133983/-/DC1

References

Atsumi, Y., Fujimori, H., Fukuda, H., Inase, A., Shinohe, K., Yoshioka, Y., Shikanai, M., Ichijima, Y., Unno, J., Mizutani, S. et al. (2011). Onset of quiescence following p53 mediated down-regulation of H2AX in normal cells. *PLoS ONE* **6**, e23432.

Bandhakavi, S., Kim, Y. M., Ro, S. H., Xie, H., Onsongo, G., Jun, C. B., Kim, D. H. and Griffin, T. J. (2010). Quantitative nuclear proteomics identifies mTOR regulation of DNA damage response. *Mol. Cell. Proteomics* **9**, 403-414.

Barascu, A., Le Chalony, C., Pennarun, G., Genet, D., Imam, N., Lopez, B. and Bertrand, P. (2012). Oxidative stress induces an ATM-independent senescence pathway through p38 MAPK-mediated lamin B1 accumulation. *EMBO J.* **31**, 1080-1094.

Bertacchini, J., Beretti, F., Cenni, V., Guida, M., Gibellini, F., Mediani, L., Marin, O., Maraldi, N. M., de Pol, A., Lattanzi, G. et al. (2013). The protein kinase Akt/PKB regulates both prelamin A degradation and Lmna gene expression. *FASEB J.* **27**, 2145-2155.

Brachner, A. and Foisner, R. (2011). Lamins reach out to novel functions in DNA damage repair. *Cell Cycle* **10**, 3426.

Burtner, C. R. and Kennedy, B. K. (2010). Progeria syndromes and ageing: what is the connection? *Nat. Rev. Mol. Cell Biol.* **11**, 567-578.

Cao, K., Graziotto, J. J., Blair, C. D., Mazzulli, J. R., Erdos, M. R., Krainc, D. and Collins, F. S. (2011). Rapamycin reverses cellular phenotypes and enhances mutant protein clearance in Hutchinson-Gilford progeria syndrome cells. *Sci. Transl. Med.* **3**, 89ra58.

Capanni, C., Mattioli, E., Columbaro, M., Lucarelli, E., Parnaik, V. K., Novelli, G., Wehnert, M., Cenni, V., Maraldi, N. M., Squarzoni, S. et al. (2005). Altered pre-lamin A processing is a common mechanism leading to lipodystrophy. *Hum. Mol. Genet.* **14**, 1489-1502.

Capanni, C., Cenni, V., Haraguchi, T., Squarzoni, S., Schüchner, S., Ogris, E., Novelli, G., Maraldi, N. M. and Lattanzi, G. (2010). Lamin A precursor induces barrier-to-autointegration factor nuclear localization. *Cell Cycle* **9**, 2600-2610.

Capanni, C., Squarzoni, S., Cenni, V., D'Apice, M. R., Gambineri, A., Novelli, G., Wehnert, M., Pasquali, R., Maraldi, N. M. and Lattanzi, G. (2012). Familial partial lipodystrophy, mandibuloacral dysplasia and restrictive dermopathy feature barrier-to-autointegration factor (BAF) nuclear redistribution. *Cell Cycle* **11**, 3568-3577.

Cenni, V., Bavelloni, A., Beretti, F., Tagliavini, F., Manzoli, L., Lattanzi, G., Maraldi, N. M., Cocco, L. and Marmiroli, S. (2011a). Ankrd2/ARPP is a novel Akt2 specific substrate and regulates myogenic differentiation upon cellular exposure to H(2)O(2). *Mol. Biol. Cell* **22**, 2946-2956.

Cenni, V., Capanni, C., Columbaro, M., Ortolani, M., D'Apice, M. R., Novelli, G., Fini, M., Marmiroli, S., Scarano, E., Maraldi, N. M. et al. (2011b). Autophagic degradation of farnesylated prelamin A as a therapeutic approach to lamin-linked progeria. *Eur. J. Histochem.* **55**, e36.

Cevenini, E., Invidia, L., Lescai, F., Salvioli, S., Tieri, P., Castellani, G. and Franceschi, C. (2008). Human models of aging and longevity. *Expert Opin. Biol. Ther.* **8**, 1393-1405.

Chevanne, M., Calia, C., Zampieri, M., Cecchinelli, B., Caldini, R., Monti, D., Bucci, L., Franceschi, C. and Caiafa, P. (2007). Oxidative DNA damage repair and parp 1 and parp 2 expression in Epstein-Barr virus-immortalized B lymphocyte cells from young subjects, old subjects, and centenarians. *Rejuvenation Res.* **10**, 191-204.

Columbaro, M., Mattioli, E., Maraldi, N. M., Ortolani, M., Gasparini, L., D'Apice, M. R., Postorivo, D., Nardone, A. M., Avnet, S., Cortelli, P. et al. (2013). Oct-1 recruitment to the nuclear envelope in adult-onset autosomal dominant leukodystrophy. *Biochim. Biophys. Acta* **1832**, 411-420.

De Cecco, M., Jeyapalan, J., Zhao, X., Tamamori-Adachi, M. and Sedivy, J. M. (2011). Nuclear protein accumulation in cellular senescence and organismal aging revealed with a novel single-cell resolution fluorescence microscopy assay. *Aging (Albany, NY)* **3**, 955-967.

Di Micco, R., Sulli, G., Dobreva, M., Liontos, M., Botrugno, O. A., Gargiulo, G., dal Zuffo, R., Matti, V., d'Ario, G., Montani, E. et al. (2011). Interplay between oncogene-induced DNA damage response and heterochromatin in senescence and cancer. *Nat. Cell Biol.* **13**, 292-302.

Dominici, S., Fiori, V., Magnani, M., Schena, E., Capanni, C., Camozzi, D., D'Apice, M. R., Le Dour, C., Auclair, M., Caron, M. et al. (2009). Different prelamin A forms accumulate in human fibroblasts: a study in experimental models and progeria. *Eur. J. Histochem.* **53**, 43-52.

Dreesen, O., Chojnowski, A., Ong, P. F., Zhao, T. Y., Common, J. E., Lunny, D., Lane, E. B., Lee, S. J., Vardy, L. A., Stewart, C. L. et al. (2013). Lamin B1 fluctuations have differential effects on cellular proliferation and senescence. *J. Cell Biol.* **200**, 605-617.

Freund, A., Laberge, R. M., Demaria, M. and Campisi, J. (2012). Lamin B1 loss is a senescence-associated biomarker. *Mol. Biol. Cell* **23**, 2066-2075.

Gonzalez-Suarez, I., Redwood, A. B., Grotsky, D. A., Neumann, M. A., Cheng, E. H., Stewart, C. L., Dusso, A. and Gonzalo, S. (2011). A new pathway that regulates 53BP1 stability implicates cathepsin L and vitamin D in DNA repair. *EMBO J.* **30**, 3383-3396.

Graziotto, J. J., Cao, K., Collins, F. S. and Krainc, D. (2012). Rapamycin activates autophagy in Hutchinson-Gilford progeria syndrome: implications for normal aging and age-dependent neurodegenerative disorders. *Autophagy* **8**, 147-151.

Han, S. and Brunet, A. (2012). Histone methylation makes its mark on longevity. *Trends Cell Biol.* **22**, 42-49.

Haque, F., Mazzeo, D., Patel, J. T., Smallwood, D. T., Ellis, J. A., Shanahan, C. M. and Shackleton, S. (2010). Mammalian SUN protein interaction networks at the inner nuclear membrane and their role in laminopathy disease processes. *J. Biol. Chem.* **285**, 3487-3498.

Ibrahim, M. X., Sayin, V. I., Akula, M. K., Liu, M., Fong, L. G., Young, S. G. and Bergo, M. O. (2013). Targeting isoprenylcysteine methylation ameliorates disease in a mouse model of progeria. *Science* **340**, 1330-1333.

Koch, C. M., Joussen, S., Schellenberg, A., Lin, Q., Zenke, M. and Wagner, W. (2012). Monitoring of cellular senescence by DNA-methylation at specific CpG sites. *Aging Cell* **11**, 366-369.

Kosar, M., Bartkova, J., Hubackova, S., Hodny, Z., Lukas, J. and Bartek, J. (2011). Senescence-associated heterochromatin foci are dispensable for cellular senescence, occur in a cell type- and insult-dependent manner and follow expression of p16(ink4a). *Cell Cycle* **10**, 457-468.

Krishnan, V., Chow, M. Z., Wang, Z., Zhang, L., Liu, B., Liu, X. and Zhou, Z. (2011). Histone H4 lysine 16 hypoacetylation is associated with defective DNA repair and premature senescence in Zmpste24-deficient mice. *Proc. Natl. Acad. Sci. USA* **108**, 12325-12330.

Kueper, T., Grune, T., Prahl, S., Lenz, H., Welge, V., Biernoth, T., Vogt, Y., Muhr, G. M., Gaemlich, A., Jung, T. et al. (2007). Vimentin is the specific target in skin glycation. Structural prerequisites, functional consequences, and role in skin aging. *J. Biol. Chem.* **282**, 23427-23436.

Lattanzi, G. (2011). Prelamin A-mediated nuclear envelope dynamics in normal and laminopathic cells. *Biochem. Soc. Trans.* **39**, 1698-1704.

Lattanzi, G., Columbaro, M., Mattioli, E., Cenni, V., Camozzi, D., Wehnert, M., Santi, S., Riccio, M., Del Coco, R., Maraldi, N. M. et al. (2007). Pre-Lamin A processing is linked to heterochromatin organization. *J. Cell. Biochem.* **102**, 1149-1159.

Liu, B., Wang, J., Chan, K. M., Tjia, W. M., Deng, W., Guan, X., Huang, J. D., Li, K. M., Chau, P. Y., Chen, D. J. et al. (2005). Genomic instability in laminopathy-based premature aging. *Nat. Med.* **11**, 780-785.

Liu, Y., Drozdov, I., Shroff, R., Beltran, L. E. and Shanahan, C. M. (2013). Prelamin A accelerates vascular calcification via activation of the DNA damage response and senescence-associated secretory phenotype in vascular smooth muscle cells. *Circ. Res.* **112**, e99-e109.

Maraldi, N. M. and Lattanzi, G. (2007). Involvement of prelamin A in laminopathies. *Crit. Rev. Eukaryot. Gene Expr.* **17**, 317-334.

Maraldi, N. M., Capanni, C., Cenni, V., Fini, M. and Lattanzi, G. (2011). Laminopathies and lamin-associated signaling pathways. *J. Cell. Biochem.* **112**, 979-992.

Marmiroli, S., Bertacchini, J., Beretti, F., Cenni, V., Guida, M., De Pol, A., Maraldi, N. M. and Lattanzi, G. (2009). A-type lamins and signaling: the PI 3-kinase/Akt pathway moves forward. *J. Cell. Physiol.* **220**, 553-561.

Matarrese, P., Tinari, A., Ascione, B., Gambardella, L., Remondini, D., Salvioli, S., Tenedini, E., Tagliafico, E., Franceschi, C. and Malorni, W. (2012). Survival features of EBV-stabilized cells from centenarians: morpho-functional and transcriptomic analyses. *Age (Dordr.)* **34**, 1341-1359.

Mattioli, E., Columbaro, M., Capanni, C., Santi, S., Maraldi, N. M., D'Apice, M. R., Novelli, G., Riccio, M., Squarzoni, S., Foisner, R. et al. (2008). Drugs affecting prelamin A processing: effects on heterochromatin organization. *Exp. Cell Res.* **314**, 453-462.

Mattioli, E., Columbaro, M., Capanni, C., Maraldi, N. M., Cenni, V., Scotlandi, K., Marino, M. T., Merlini, L., Squarzoni, S. and Lattanzi, G. (2011). Prelamin A-mediated recruitment of SUN1 to the nuclear envelope directs nuclear positioning in human muscle. *Cell Death Differ.* **18**, 1305-1315.

Muñoz-Najar, U. and Sedivy, J. M. (2011). Epigenetic control of aging. *Antioxid. Redox Signal.* **14**, 241-259.

Muteliefu, G., Shimizu, H., Enomoto, A., Nishijima, F., Takahashi, M. and Niwa, T. (2012). Indoxyl sulfate promotes vascular smooth muscle cell senescence with upregulation of p53, p21, and prelamin A through oxidative stress. *Am. J. Physiol.* **303**, C126-C134.

Pospelova, T. V., Leontieva, O. V., Bykova, T. V., Zubova, S. G., Pospelov, V. A. and Blagosklonny, M. V. (2012). Suppression of replicative senescence by rapamycin in rodent embryonic cells. *Cell Cycle* **11**, 2402-2407.

Ragnauth, C. D., Warren, D. T., Liu, Y., McNair, R., Tajsic, T., Figg, N., Shroff, R., Skepper, J. and Shanahan, C. M. (2010). Prelamin A acts to accelerate smooth muscle cell senescence and is a novel biomarker of human vascular aging. *Circulation* **121**, 2200-2210.

Ramos, F. J., Chen, S. C., Garelick, M. G., Dai, D. F., Liao, C. Y., Schreiber, K. H., MacKay, V. L., An, E. H., Strong, R., Ladiges, W. C. et al. (2012). Rapamycin reverses elevated mTORC1 signaling in lamin A/C-deficient mice, rescues cardiac and skeletal muscle function, and extends survival. *Sci. Transl. Med.* **4**, 144ra103.

Richards, S. A., Muter, J., Ritchie, P., Lattanzi, G. and Hutchison, C. J. (2011). The accumulation of un-repairable DNA damage in laminopathy progeria fibroblasts is caused by ROS generation and is prevented by treatment with N-acetyl cysteine. *Hum. Mol. Genet.* **20**, 3997-4004.

Schellenberg, A., Lin, Q., Schüler, H., Koch, C. M., Joussen, S., Denecke, B., Walenda, G., Pallua, N., Suschek, C. V., Zenke, M. et al. (2011). Replicative senescence of mesenchymal stem cells causes DNA-methylation changes which correlate with repressive histone marks. *Aging (Albany, NY)* **3**, 873-888.

Shimi, T., Butin-Israeli, V., Adam, S. A., Hamanaka, R. B., Goldman, A. E., Lucas, C. A., Shumaker, D. K., Kosak, S. T., Chandel, N. S. and Goldman, R. D. (2011). The role of nuclear lamin B1 in cell proliferation and senescence. *Genes Dev.* **25**, 2579-2593.

Sikora, E., Arendt, T., Bennett, M. and Narita, M. (2011). Impact of cellular senescence signature on ageing research. *Ageing Res. Rev.* **10**, 146-152.

Journal of Cell Science (2014) 127, 147–157 doi:10.1242/jcs.133983

Tesco, G., Vergelli, M., Grassilli, E., Salomoni, P., Bellesia, E., Sikora, E., Radziszewska, E., Barbieri, D., Latorraca, S., Fagiolo, U. et al. (1998). Growth properties and growth factor responsiveness in skin fibroblasts from centenarians. *Biochem. Biophys. Res. Commun.* **244**, 912-916.

Ukekawa, R., Miki, K., Fujii, M., Hirano, H. and Ayusawa, D. (2007). Accumulation of multiple forms of lamin A with down-regulation of FACE-1 suppresses growth in senescent human cells. *Genes Cells* **12**, 397-406.

Wilkinson, J. E., Burmeister, L., Brooks, S. V., Chan, C. C., Friedline, S., Harrison, D. E., Hejtmancik, J. F., Nadon, N., Strong, R., Wood, L. K. et al. (2012). Rapamycin slows aging in mice. *Aging Cell* **11**, 675-682.

Zironi, I., Gaibani, P., Remondini, D., Salvioli, S., Altilia, S., Pierini, M., Aicardi, G., Verondini, E., Milanesi, L., Bersani, F. et al. (2010). Molecular remodeling of potassium channels in fibroblasts from centenarians: a marker of longevity? *Mech. Ageing Dev.* **131**, 674-681.